Order−Disorder Transitions and Evolution of Silica Structure in Self-Assembled Mesostructured Silica Films Studied through FTIR Spectroscopy

Plinio Innocenzi* and Paolo Falcaro

Dipartimento di Ingegneria Meccanica, settore materiali, Università di Padova, via Marzolo 9, 35131 Padova, Italy

David Grosso and Florence Babonneau

Chimie de la Matière Condensée, Université Paris 6-T54-E5, 4 place Jussieu, 75252 Paris Cedex 05, France

Received: July 25, 2002; In Final Form: February 20, 2003

Silica mesoporous thin films have been synthesized with a self-assembling process using cetyltrimethylammonium bromide as an organic template and tetraethyl orthosilicate as the silica source. Mesoporous films with *Pm*3*n* cubic phase have been obtained and the films have been thermally treated in air with a progressive heating schedule from as-deposited up to 1000 °C. The evolution of silica network has been studied with transmission Fourier transformed infrared (FTIR) spectroscopy. The presence of cyclic species in the precursor solution has been shown by ^{29}Si nuclear magnetic resonance (NMR) experiments. FTIR spectra of as-deposited films have shown that some of these cyclic species are retained in the structure after film deposition, but at temperatures larger than 350 °C they have been no longer observed. In the 1000−1300 cm^{-1} region, several overlapped absorption bands have been detected. In particular, the LO_3−TO_3 pair, the cyclic species absorption bands and the LO_4−TO_4 pair have been resolved. These last bands are associated with disorder−order transitions in the silica structure. These disorder-induced optical modes are due to the large interface area in mesoporous silica films and related to bond strains. The evolution of the bands in the 1000−1300 cm^{-1} region has been followed with the Berreman configuration, performing the transmission FTIR analysis at 45° with respect to the normal incidence angle. The LO_3 band, which in silica sol−gel films is indicative of network condensation and is enhanced by scattering of the light in the pores, has been resolved as a single sharp band from 250 °C.

1. Introduction

Infrared (IR) spectroscopy has been widely used in the last years to characterize the different stages from sols to gels and glasses.[1−8] IR spectra have been correlated to structure and composition of different types of sol−gel materials, especially sol−gel derived silica glasses, which have been the subject of extensive specific investigations. Detailed studies by IR spectroscopy have been reported on sol−gel processing of silica glasses, in particular on the formation of oligomeric species during the hydrolysis−polycondensation of silicon alkoxides,[1] on evolution of the alkoxides to silica gels and glasses,[2] on silica xerogels,[3−5] and on structural changes of silica gels in the early stages of their conversion to glasses.[6,7]

More recently new silica materials with a mesostructured organization have been synthesized via surfactant templating supramolecular chemistry.[9−13] Mesoporous materials have been obtained as powders for a large variety of oxides, while thin oxide films have been more difficult to fabricate, because of the need for a strict control of the experimental parameters during the evaporation-induced self-assembly (EISA) process that governs the mesophase formation during film deposition.[14] Many efforts have been addressed for the preparation of such mesoporous silica films on glass or silicon substrates using sol−gel chemistry in conjunction with ionic or nonionic surfactants.[15,16] Films with different mesoporous geometries, such as cubic, 2D-hexagonal, or 3D-hexagonal, have been obtained depending on the synthesis conditions. Detailed structural studies have been carried out by Klotz[17] et al. and by Grosso[18] et al. using 1-D and 2-D X-ray scattering techniques and transmission electron microscopy to describe the film structure. In particular, the mechanism of film formation has been clarified by in-situ time-resolved small-angle X-ray scattering experiments.[18]

While most of the research has been focused on the characterization and control of the types of mesostructures as a function of the different synthesis parameters, it is not yet well-established how the overall synthesis process affects the microstructure of the silica walls that form the porous material skeleton. FTIR spectroscopy has thus been used to study the structural changes in the silica network during the different stages of the film thermal curing.

2. Experimental Section

A stock solution was first prepared by refluxing for 90 min tetraethyl orthosilicate (TEOS) dissolved in ethanol (EtOH) with H_2O and HCl as acid catalyst. The molar ratios were TEOS/EtOH/H_2O/HCl = 1:3:1:0.00005. A second solution was prepared with cetyltrimethylammonium bromide ($C_{16}H_{33}(CH_3)_3N^+Br^-$, (CTAB)), EtOH, H_2O, and HCl, and slowly added to the stock sol; the final molar ratios were TEOS/EtOH/H_2O/HCl/CTAB = 1:20:5:0.004:0.14. The solution was finally stirred at room temperature for 5 days.

Thin films were deposited by dip-coating on one side polished (100) silicon substrates in a humidity-controlled box at 30%

* Corresponding author.

10.1021/jp026609z CCC: $25.00
Published on Web 04/26/2003

RH. The films were calcined in air for 15 min at different temperatures from 50 to 900 °C. The samples were directly inserted in the preheated oven at the selected temperature of annealing.

The films were characterized by low angle X-ray diffraction on a Philips PW 1830 diffractometer with Ni-filtered Cu Kα radiation ($\lambda = 1.5418$ Å). A $\theta-2\theta$ geometry for thin film analysis was used. Data were collected from 1.5 to 10° in 2θ with a 0.02° step and a sampling interval of 5 s. A 1/6 mm width slit was used on the detector. The voltage was 40 kV, and the current was 30 mA.

The film thickness was measured by a profilometer (Alpha Step 200, Tencor Instruments). The typical thickness of the film was in the range 150−350 nm, depending on the temperature of calcination and annealing.

Fourier transform infrared (FTIR) absorption spectra, in the range 4500−400 cm^{-1}, were recorded using a Perkin-Elmer 2000 spectrophotometer. The spectra were obtained in transmission from the films deposited on silicon substrate, which is IR transparent, with an accuracy of ± 0.5 cm^{-1}; each spectrum was the result of 24 scans. FTIR spectra were also acquired in transmission with incidence angles of 45° and 65°.

A Gaussian peak fitting procedure has been applied to the FTIR spectra (Microcal Origin Software); the quality of the fitting was evaluated on the basis of the χ^2-values (in the order of 10^{-6}) and correlation coefficient values = 0.998.

The ^{29}Si solution state NMR spectra were recorded on a MSL400 Bruker spectrometer at 79.5 MHz. The sample was held in an 8 mm tube that was in turn placed in a 10 mm tube with C_6D_6 in the annulus as lock solvent. The pulse width was 12.8 μs (90° pulse), and the recycle delay was 60 s. The background peak due to the tube and/or the probe at −110 ppm (Q_4 site) has been subtracted. The Si sites will be labeled using the usual Q_i nomenclature, where *i* represents the number of oxo bridges bonded to the given Si.

3. Results

As previously mentioned in the literature, the best organization for films prepared via EISA occurs when the starting sol is aged for several days.[18] This is the reason the films described in this work have been prepared with sols aged for 5 days.

The evolution of the Si species during this aging step has been followed by ^{29}Si NMR (Figure 1). After 2 h, the main peaks at −82, −84, −86, −88 ppm (Q_1 sites) and −95 ppm (Q_2 sites) are mainly characteristic of short linear species.[19] After 12 h, the peaks due to Q_1 end groups have decreased in favor of peaks at −90.8 and −92.9 ppm which can be assigned to the formation of four-member ring cyclic species [$(\equiv SiO)_2Si(OH)_2$ and $(\equiv SiO)_2Si(OH)(OEt)$ sites, respectively]. After 2 days, these peaks are dominant, while those due to Q_1 species have almost disappeared, and a new peak at −99.4 ppm due to Q_3 sites is now present due to branching. After 5 days, 3 main peaks remained due to Q_2 cyclic species and Q_3 branching sites. The low angle XRD (LAXRD) patterns of as-deposited films showed a *Pm*3*n* cubic structure, (Figure 2) which remained stable up to around 800 °C. The presence of the three 200, 210, and 211 peaks revealed that the organized domains are preferentially oriented with their (200) or (210) or (211) directions normal to the substrate.[17,20] The relative unidirectional contraction of the domains, calculated from the LAXRD patterns, with thermal curing are shown in the inset of Figure 2. At 900 °C, a 55% relative contraction ($d_o - d/d_o$) is observed. This effect is generally observed in mesoporous films upon thermal calcination and is due to condensation of the inorganic network.

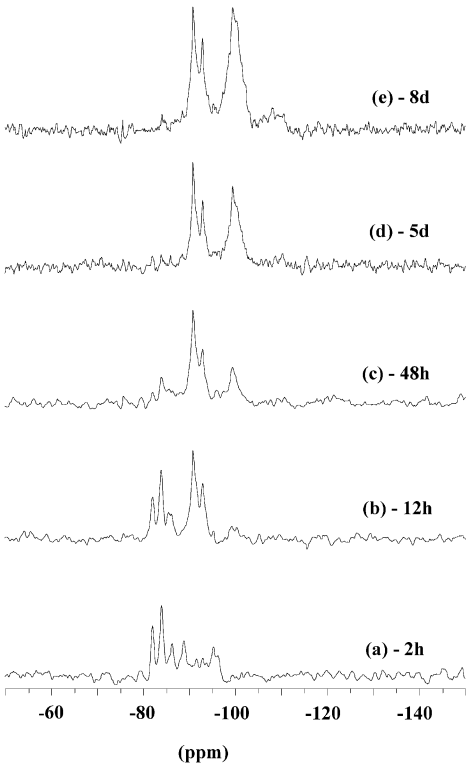

Figure 1. ^{29}Si NMR spectra of the sol after various aging times: (a) 2 h, (b) 12 h, (c) 48 h, (d) 5 days, and (e) 8 days.

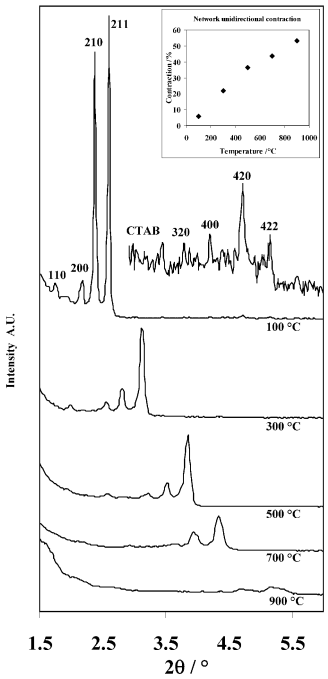

Figure 2. LAXRD patterns of *Pm*3*n* structured films thermally treated from 100 to 900 °C. Inset: relative unidirectional contraction of the domains with temperature.

The FTIR spectrum in the 4500−450 cm^{-1} range of an as-deposited film is shown in Figure 3. The spectrum shows several different features attributed to silica, the templating cationic surfactant, and residual water.

The presence of CTAB is characterized by two intense absorption bands assigned to asymmetric (∼2980 cm^{-1}) and symmetric (∼2850 cm^{-1}) stretching vibrations of $C-CH_2$ in the CTAB chain.[21] The absorption energies of CH_2 stretching

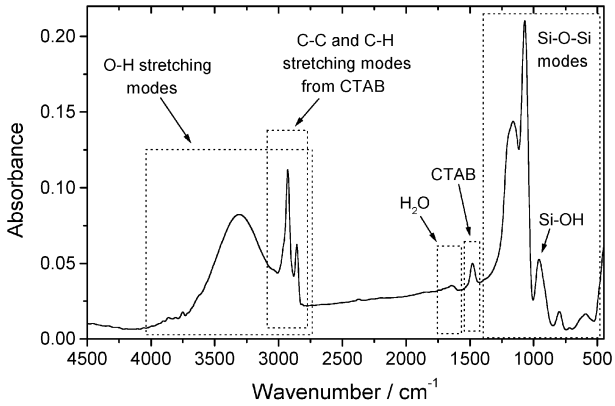

Figure 3. Absorption FTIR spectrum of an as-deposited mesoporous silica film deposited by dip-coating on silicon substrate.

vibrations are considered to be related with the physical state (monomer, micelle, or solid) of the surfactant (see ref 21 and references therein). In Figure 3 the CH_2 vibrational energies are found at 2857 and 2927 cm^{-1}, indicating that the surfactant is present in the film as micelles. This is also supported by the absence of several weak bands in the region from 2940 to 2960 cm^{-1} that are assigned to C−CH_3 asymmetric stretching and N−CH_3 symmetric stretching vibrations of the solid surfactant.[21]

The three main peaks characteristic of Si−O−Si bonds vibrational modes[22] are detected around 1070, 800, and 460 cm^{-1}. The lowest frequency mode (∼460 cm^{-1}) is assigned to transverse optical rocking motions (TO_1 mode). Near 800 cm^{-1}, a weak band due to Si−O−Si symmetric stretching (TO_2 mode) is observed. The highest frequency mode around 1070 cm^{-1}, whose intensity is the largest one, is assigned to antisymmetric stretching (TO_3 mode). The TO_3 band appears generally accompanied by an intense shoulder at the high frequency side; in the present case the shoulder is instead substituted by an intense peak with definite features. The nature of this band and its evolution with temperature will be specifically discussed later on. Another vibrational mode is detected around 600 cm^{-1}, and there is good agreement in the literature to attribute this distinct weak and broad band, generally observed in sol−gel silica materials, to residual cyclic structures present in the silica network. Yoshino et al.[23] have assigned this IR vibration to cyclic tetrameric siloxane species by referring to different types of cyclic siloxanes and silicate minerals, and this attribution has been recently supported by molecular orbital calculations.[24] This vibration mode was assigned to a four-member ring within the ring plane: the Si−O stretching vibration coupled with O−Si−O and Si−O−Si bending vibrations.[23]

A band of medium intensity centered near 940−960 cm^{-1} is attributed to Si−OH stretching vibrations.[25,26] This band is, however, not univocally assigned because it can overlap or coincide with Si−O$^-$, Si−O−C (from unhydrolyzed OEt groups), and several vibrations from residual CTAB.

A broad intense band is detected between 2800 and 4000 cm^{-1}, due to O−H vibrations from different species. On a literature basis (refs 27−29, and references therein), two main groups of bands can be found in this interval: around 3800−3650 cm^{-1}, stretching modes of isolated OH groups[30] around ∼3740 cm^{-1} or OH groups partially involved in hydrogen bonding and around 3650−3200 cm^{-1}, stretching modes of strongly hydrogen-bonded OH groups in chains of different lengths.

Figure 4 shows the evolution with temperature of the mesostructured silica film FTIR absorption spectra (750−1750 cm^{-1} region). An increase in intensity of the Si−O−Si

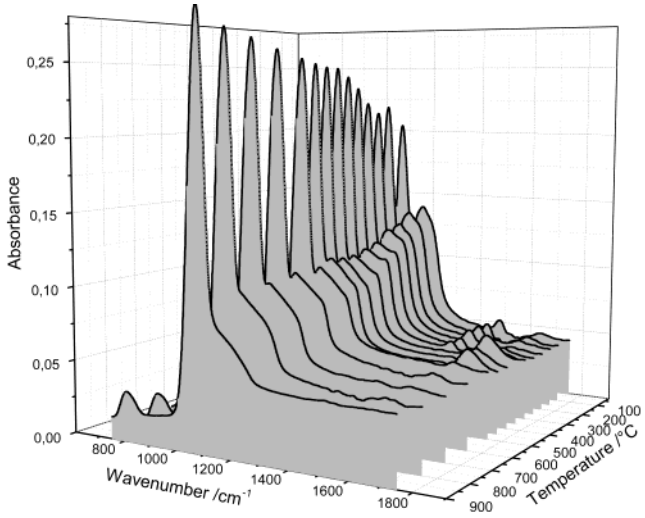

Figure 4. 3-D view of FTIR absorption spectra, in the range 750−1750 cm^{-1}, of silica mesoporous films as a function of firing temperature.

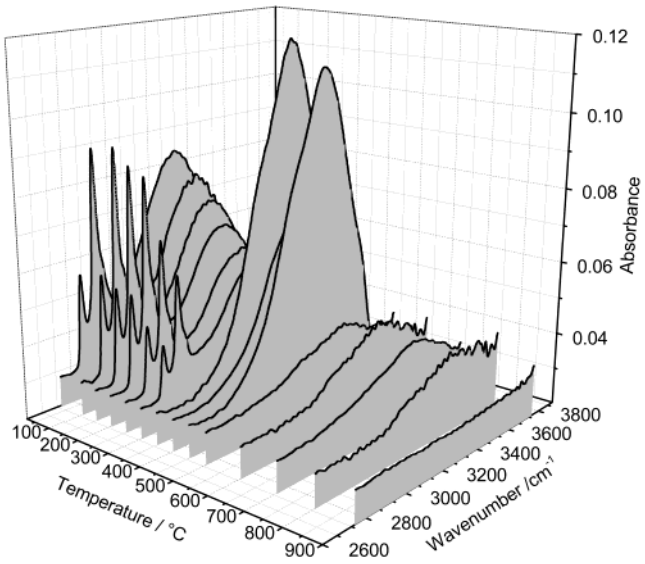

Figure 5. 3-D view of FTIR absorption spectra, in the range 2850−3650 cm^{-1}, of silica mesoporous films as a function of firing temperature.

antisymmetric stretching mode (TO_3) is accompanied by a decrease of the peak around 1200 cm^{-1} that disappears at 800 °C. The intensity of the band due to residual CTAB (∼1400 cm^{-1}) decreases, and after a thermal treatment at 400 °C this band disappears. The decrease of this band is similarly accompanied by a decrease of the molecular water band, which, however, suddenly increases in intensity when CTAB is removed . This relationship between water and CTAB in the mesostructured film is clearly observed in the FTIR spectra of the 2800−4000 cm^{-1} region. Figure 5 shows the evolution during thermal treatment of the CTAB vibrational modes (the two sharp intense peaks at 2980 and 2850 cm^{-1}) and of the hydroxyl band. When the templating surfactant CTAB is removed from the mesostructure (at 350 °C), a sudden increase in intensity of the O−H stretching band is observed. This OH band disappears from the spectra only after thermal treatment at 900 °C.

The changes with temperature of the ∼1200 cm^{-1} peak on the high-frequency side of the TO_3 mode are shown in Figure 6. This band is indeed composed of several different overlapping

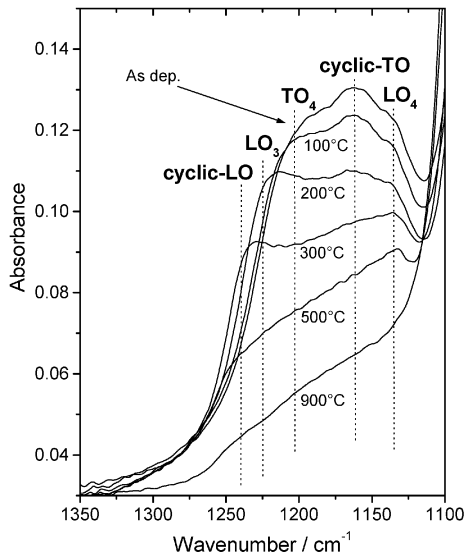

Figure 6. FTIR absorption spectra, in the range 1100−1350 cm^{-1}, of silica mesoporous films treated at different temperatures.

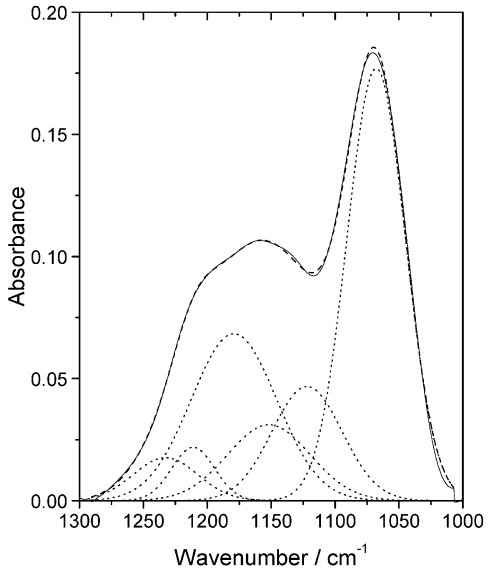

Figure 7. Deconvolution of the FTIR absorption spectrum, in the 1100−1300 cm^{-1} interval, for an as-deposited mesoporous silica film.

components. Attribution of these modes in sol−gel silica films is somehow a controversial question. According to the literature, the following assignments can be made: the LO_3 mode located at 1220−1250 cm^{-1}, a fourth LO−TO pair at ∼1190 cm^{-1} (TO_4) and at ∼1130 cm^{-1} (LO_4), and a LO−TO pair assigned to antisymmetric stretching (Si−O−Si) in strained 4-fold siloxane rings.[31] These bands show different evolutions during the thermal treatment. The band of cyclic species disappears at 400 °C, similarly to the band at 600 cm^{-1} also assigned to 4-fold rings, the LO_4 band disappears at 800 °C, and the LO_3 mode decreases in intensity with higher temperatures of treatment. The TO_4 mode is not directly detected and is assigned on the basis of the literature.

Deconvolution of the FTIR spectra in the interval ≈1000−1300 cm^{-1} relative to as-deposited films has been performed considering six different vibrational modes: LO_3 and TO_3, LO_4 and TO_4, and TO and LO in strained 4-fold rings. The result of the deconvolution is shown in Figure 7; a good fit is achieved with six Gaussian curves. On the basis of the deconvolution, the different vibrational modes are detected at 1068 (TO_3), 1180 (LO_3), 1120 (LO_4), 1210 (TO_4), 1151 (4-f. TO), and 1232 (4-f. LO) cm^{-1}. The FTIR spectra detected with an incidence angle of 45° are shown in Figure 8. They show a strong enhancement of the longitudinal optical modes, especially LO_3 that appears as an intense peak at 1240−1250 cm^{-1}. The intensity peak due to the LO_4 mode is also enhanced up to 800 °C, but it disappears at 900 °C (Figure 9). The thermal treatment causes a shift in frequency of the TO_3 mode (Figure 10), which shows a slight decrease up to 200 °C with a first minimum, then an increase in frequency up to 400 °C with a new minimum around 500 °C, and after this temperature the frequency steadily increases again up to 900 °C.

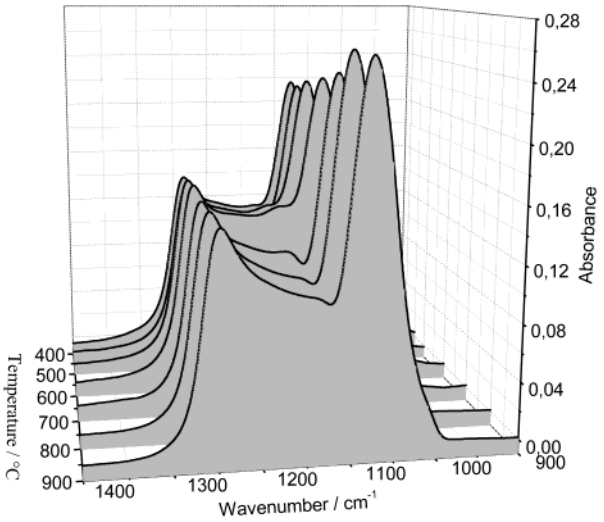

Figure 8. 3-D view of FTIR absorption spectra, in the range 800−1750 cm^{-1}, of silica mesoporous films treated at different temperatures. The spectra are detected at an angle of 45° of oblique incidence.

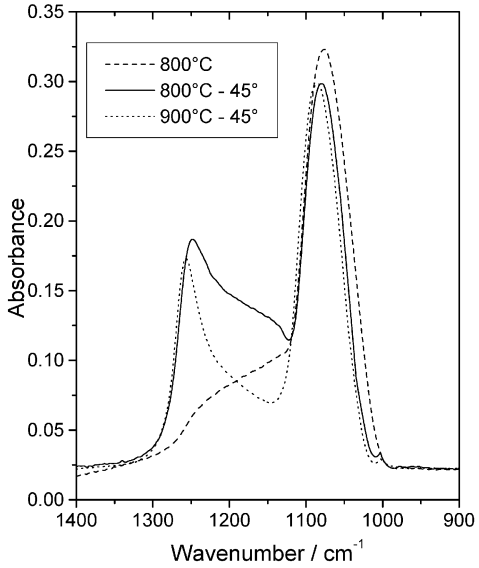

Figure 9. FTIR absorption spectra, in the range 900−1400 cm^{-1}, of silica mesoporous films treated at 800 °C (normal incidence) and 800 and 900 °C (45° oblique incidence).

A shift in the absorption maxima of the hydroxyl band around 3500 cm^{-1} is also induced by the thermal treatment (Figure 11). After calcination and full removal of CTAB from the silica mesoporous film, the absorption spectrum shows different features with a main peak located at 3428 cm^{-1} due to hydrogen-bonded Si−OH in chains, a shoulder near 3250 cm^{-1} due to absorbed molecular water, and a shoulder near 3635 cm^{-1} due to terminal silanol species.

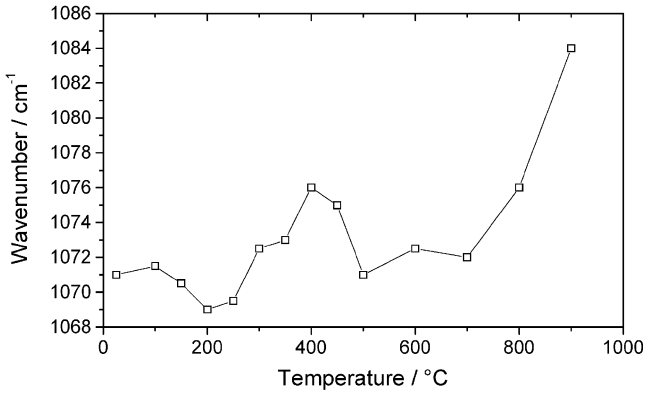

Figure 10. Shift as a function of the temperature of the TO_3 (~1070 cm^{-1}) vibration mode.

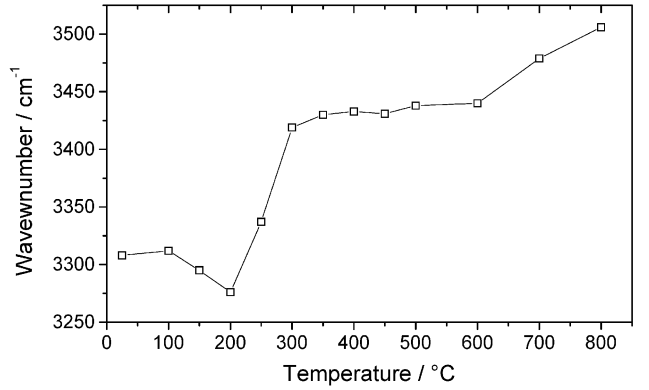

Figure 11. Shift as a function of the temperature of the hydroxyl band around 3500 cm^{-1} as a function of the thermal treatment temperature.

4. Discussion

Presence of Cyclic Species. The formation of cyclic species during the early stages of the hydrolysis and condensation of TEOS in the precursor sol is directly related to the synthesis conditions (H_2O/alkoxide ratio and pH).[32] In the present synthesis, with $H_2O/TEOS = 1$ in acidic condition, the formation of four-member ring cyclic species has been observed in the sol by ^{29}Si NMR, after several aging days. Indeed, the best organization of the mesostructured films seems related to the presence of a large number of such cyclic species in the sol.[33,34] Larger size rings may be present, but cannot be clearly identified from the NMR spectra.

Fully densified sol−gel silica glasses have a microstructure similar to that of melt-derived silica glasses, and the basic ring units are formed by 6-fold siloxane rings. At different drying and firing stages, IR spectra of sol−gel silica materials show evidence of cyclic species retained in the structure,[23] in particular the bands at 600 and 1200 cm^{-1} have been attributed to 4-fold siloxane rings. The presence of these bands is deduced by the FTIR spectra of as-deposited mesoporous silica films (Figure 3) and the deconvolution of this spectrum (Figure 7); their retention in the microstructure from the precursor sol is, therefore, well supported. The 4-fold rings are also observed to evolve with thermal treatment: in the literature, it is commonly observed that the bands related to cyclic species disappear when sol−gel silica is heated at temperatures larger than 300 °C.[7] A similar evolution is also observed in the silica mesoporous films, where the bands due to cyclic species are no longer observed when the calcination temperature is larger than 350 °C (Figure 6).

Structural Evolution of the Silica Walls with Temperature. One of the effects induced by the thermal treatment, as observed in the previous paragraph, is a rearrangement of the 4-fold species in the silica structure at temperatures lower than 300 °C. In these mesoporous films the silica tetrahedra form the building blocks in the mesostructured organization of the material. Even after the pore collapse the film retains a residual porosity[16] that has, however, lost any topological organization and full densification is achieved only at temperatures larger than 800 °C. The thermal process induces the condensation of silica that forms the pore walls and at the same time causes the shrinkage of the pores and finally their collapse. The model of the central force network of Sen and Thorpe[35] and Galeener,[36] as suggested by Almeida,[26] can be applied to explain the shift of the TO_3 mode in silica sol−gel films. In this model, the TO_3 asymmetric stretching frequency, ω, is related to the Si−O−Si intertetrahedral bond angle, θ, and to the Si−O stretching force constant, k, by the following expression:

$$\omega^2 = \frac{k}{m_O}(1 - \cos\theta) + \frac{4}{3}\frac{k}{m_{Si}} \quad (1)$$

where m_O and m_{Si} are the mass of the oxygen and silicon atoms, respectively. While an increase in the Si−O−Si angle, θ, increases the frequency vibration, on the other hand, an increase in the Si−O bond length leads to a decrease in k and a shift in the opposite direction. Thus, the shift of the TO_3 vibration mode to lower wavenumbers is related to a predominance of the Si−O bond tensile strain effect over that of the bridging angle increase, which is indicative of an increase in the porosity volume fraction. The Si−O−Si bridges being strained near the surface of the gel pores, with larger bridging angles and slightly longer Si−O bonds, with a predominance of the bond effect, may explain this.

The shift to lower wavenumbers is, therefore, related to a more porous structure with smaller siloxane rings, larger Si−O−Si angles, and Si−O bond lengths. These two effects, following the central force model, can combine to lead to a decrease in the Si−O stretching constant.

FTIR spectra of sol−gel silica films recorded as a function of the firing temperature show, usually between 400 and 500 °C, a decrease of the TO_3 mode to a minimum value, and then, an increase to larger frequency. The minimum was correlated to a maximum in porosity that occurs after the drying stage,[37] when the pores are emptied of water and residual solvent. In mesoporous silica films two minima are observed (Figure 10) around 200 °C, corresponding to the first drying stages with the removal of molecular water and ethanol and a second one after calcination of the cationic template. After 600 °C, densification via viscous sintering of the film starts with collapse of the mesostructure, which is almost completed at 900 °C.

A better observation of the LO vibrational modes in the 1300−1000 cm^{-1} region is observed at oblique incidence of the IR radiation (Figure 8). LO modes, in fact, cannot be observed in normal incidence infrared absorption spectra, because they do not interact directly with the incident light; however, they can be detected in oblique-incidence, due to the Berreman effect.[38] In particular, the intensity of the LO_3 mode near 1250 cm^{-1} is strongly enhanced in this geometry. Several experiments done at oblique incidence of the IR beam in silica sol−gel films have shown an enhancement of the LO_3 mode intensity.[39] The nature of the ~1250 cm^{-1} shoulder at normal incidence has been explained by Almeida and Pantano[26] as a broadened signature of the LO component of the TO_3 asymmetric stretching, or a mixed LO−TO mode with dominant LO

character. The observation of this shoulder is thus much enhanced at a larger pore volume. The intensity of this mode is observed to increase with porosity because of the scattering of the infrared radiation within the pores and the consequent activation of the LO modes. The large porosities in mesoporous films explain the observed large intensity of the LO_3 mode even at normal incidence. A significant change in shape and intensity of the 1250 cm^{-1} shoulder is observed at 600 °C with the collapse of the mesostructure.

Disorder-Induced Modes. FTIR absorption spectra of amorphous silica films typically show three major TO (transverse optical) absorption bands that are associated with a particular vibrational mode of the bridging oxygen atoms, O, with respect to the silicon atom pair they are bonded to. The presence of a fourth TO_4 absorption band has been demonstrated by Kirk[40] and associated with disorder-induced vibrational mode coupling in thin amorphous silica films. Paired with each one of these four TO modes, there is a longitudinal optical (LO) mode, which gives rise to the known LO−TO split.[41] The frequency of these LO vibrational modes is larger than in their paired TO modes, with the exception of the LO_4-TO_4 pair.

Experimental evidence of this LO_4-TO_4 inverted mode has been reported for different types of silica thin films[42−44] and correlated to an increased disorder in the structure, as a result of an increase in bond strain.

Clear observations of the LO_4 vibrational mode is very difficult in oxide films if the IR analysis is not performed at oblique incidence and if the films are not thin enough. The detection of LO_4, because of its disorder-induced nature, seems also very sensitive to the preparation conditions. It has been reported in sol−gel films,[39,45] but basically deduced only on the basis of deconvolution curves, and widely discussed by Lange for different types of SiO_2 thin films.[42−44] It is important to observe that an increase in intensity at oblique incidence must be detected to be sure of the detection and attribution of the LO_4 mode. In fact, the longitudinal nature of this vibration should produce an enhancement of the mode intensity due to the Berreman effect. Furthermore, the band should not be confused with the vibrational modes of cyclic species that are present in the same spectral region. In the mesoporous films from 300 °C (Figure 6), the LO_4 mode is detected around 1130 cm^{-1} with normal incidence and the band shows a strong enhancement when the analysis is done at oblique incidence (Figures 8 and 9). This enhancement in intensity of the LO_4 mode is observed in the spectra of the films fired at 800 °C, because in the spectrum at normal incidence the LO_4 vibration is not observed while it is detected in the same film at oblique incidence.

The evolution with temperature of the LO_4 mode shows a decrease in intensity when the temperature increases, suggesting a change to a more ordered structure. The transition to order is completed after firing at 900 °C. The nature of the disorder is related to a large pore volume in mesostructured silica films, characterized by a very large surface, where the silica bonds are strained. This is the first direct experimental evidence, to the knowledge of the authors, of the presence of disorder-induced LO_4 modes in silica sol−gel or surfactant-templated mesoporous silica films.

Dehydroxylation. The thermal treatment causes the calcination of the surfactant that is completely removed from the film at 350 °C and the condensation of the silanols with elimination of water. As a consequence the length of the hydrogen-bonded chains decreases while the isolated species increase. This explains the gradual shift to high frequency of the OH···O groups band during dehydroxylation (Figure 11). The calcination process produces a discontinuity in this dehydroxylation process: when the hydrophobic surfactant molecules are totally removed, the large surface area is then covered by silanol species, which immediately adsorb molecular water, as revealed by the abrupt increase of the signals at 1640 and 3300 cm^{-1}.[46,47] These data are well in accordance with what was observed during thermal degradation of CTAB in MCM-41 powders.[48] It is also interesting to observe that full density in mesoporous silica films is reached for temperatures larger than those necessary for conventional sol−gel silica films.[26]

5. Conclusions

The FTIR spectra of *Pm*3*n* cubic mesoporous silica films prepared using cetyltrimethylammonium bromide as cationic surfactant show several specific features that are correlated to the organized structure and the large porosity of the material. The spectra detected at different temperatures have allowed us to follow the changes in the microstructure during the different stages of the film preparation, immediately after deposition, during drying, calcination, and densification. In particular, 4-fold cyclic species are retained in the silica walls of the pores from the precursor sol up to 300 °C; this species is linked to the absorption bands observed at 600 and 1200 cm^{-1} that show a similar evolution with the temperature.

Experimental evidence of a disorder-induced mode coupling has been found through the detection of a longitudinal transversal optical mode (LO_4); the transition goes to completion around 800 °C. These disorder-induced optical modes are due to the presence of a large interface area and likely are related to bond strains.

The shift of the antisymmetric stretching (TO_3) band can be used to observe the evolution of the porosity during the thermal treatment with the temperature. Evaporation of residual water and solvent causes a first decrease in porosity, followed by an enhancement in porosity and a new decrease in porosity after calcination and a continuous porosity decrease up to the film condensation.

Different stages in the dehydroxylation process are also observed, a first one until the surfactant is completely removed and immediately after when a very large adsorption of molecular water is observed. Full dexydroxylation requires large temperatures, up to 800 °C.

Acknowledgment. Prof. Rui Almeida, (Departamento de Engenharia de Materiais/INESC, Lisboa Portugal), is gratefully acknowledged for helpful discussions.

References and Notes

(1) Gnado, J.; Dhamelincourt, P.; Pelegris, C.; Traisnel, M.; Le Maguer Mayot, A. *J. Non-Cryst. Solids* **1996**, *208*, 247.

(2) Matos, M. C.; Ilharco, L. M.; Almeida, R. M. *J. Non-Cryst. Solids* **1992**, *147&148*, 232.

(3) Wood, D. L.; Rabinovich, E. M. *J. Non-Cryst. Solids* **1986**, *82*, 171.

(4) Wood, D. L.; Rabinovich, E. M. *Appl. Spectrosc.* **1989**, *43*, 263.

(5) Almeida, R. M.; Guiton, T. A.; Pantano, G. C. *J. Non-Cryst. Solids* **1990**, *121*, 193.

(6) Bertoluzza, A.; Fagnano, C.; Morelli, M. A.; Gottardi, V.; Guglielmi, M. *J. Non-Cryst. Solids* **1982**, *48*, 117.

(7) Yoshino, H.; Kamiya, K.; Nasu, H. *J. Non-Cryst. Solids* **1990**, *126*, 68.

(8) Innocenzi, P. *J. Non-Cryst. Solids* **2003**, *316*, 309.

(9) Beck, J. S.; Vartuli, J. C.; Roth, W. J.; Leonowicz, M. E.; Kresge, C. T.; Schmitt, K. D.; Chu, C. T.-W.; Olson, D. H.; Sheppard, E. W.; McCullen, S. B.; Higgins, J. B.; Schlenker, J. L. *J. Am. Chem. Soc.* **1992**, *114*, 10834−10842.

(10) Huo, Q.; Margolese, D. J. I.; Ciesla, U.; Demuth, D. G.; Feng, P.; Gier, T. E.; Sieger, P.; Firouzi, A.; Chmelka, B. F.; Schüth, F.; Stucky, G. D. *Chem. Mater*. **1994**, *6*, 1176.
(11) Huo, Q.; Margolese, D. I.; Stucky, G. D. *Chem. Mater*. **1996**, *8*, 1147.
(12) Melosh, N. A.; Lipic, P.; Bates, F. S.; Wudl, F.; Stucky, G. D.; Fredrickson, G. H.; Chmelka, B. F. *Macromolecules* **1999**, *32*, 4332.
(13) Ying, J. Y.; Mehnert, C. P.; Wong, M. S. *Angew. Chem., Int. Ed. Engl*. **1999**, *38*, 56.
(14) Brinker, C. J.; Lu, Y.; Sellinger, A.; Fan, H. *Adv. Mater*. **1999**, *11*, 579.
(15) Zhao, D.; Yang, P.; Melosh, N.; Chmelka, B. F.; Stucky, G. D. *Adv. Mater*. **1998**, *10*, 1380.
(16) Grosso, D.; Balkenende, A. R.; Albouy, P. A.; Lavergne, M.; Mazerolles, L.; Babonneau, F. *J. Mater. Chem*. **2000**, *10*, 2085.
(17) Klotz, M.; Albouy, P. A.; Ayral, A.; Menager, C.; Grosso, D.; Van der Lee, A.; Cabuil, V.; Babonneau, F.; Guizard, C. *Chem. Mater*. **2000**, *12*, 1721.
(18) Grosso, D.; Balkenende, A. R.; Albouy, P. A.; Ayral, A.; Amenitsch, H.; Babonneau, F. *Chem. Mater*. **2001**, *13*, 1848.
(19) Hunger, B.; Jancke, H.; Hähnert, M.; Stade, H. *J. Sol-Gel Sci. Technol*. **1994**, *2*, 51.
(20) Soler-Illia, G. J.; Crepaldi, E. L.; Grosso, D.; Durand, D.; Sanchez, C. *Chem. Commun.* **2002**, 2298.
(21) Kung, K. H. S.; Hayes, K. F. *Langmuir* **1993**, *9*, 263.
(22) Galeener, F. L. *Phys. Rev. B* **1979**, *19*, 4292.
(23) Yoshino, H.; Kamiya, K.; Nasu, H. *J. Non-Cryst. Solids* **1990**, *126*, 68.
(24) Hayakawa S.; Hench, L. L. *J. Non-Cryst. Solids* **2000**, *262*, 264.
(25) Bertoluzza, A.; Fagnano, C.; Morelli, M. A.; Gottardi, V.; Guglielmi, M. *J. Non-Cryst. Solids* **1982**, *48*, 117.
(26) Almeida, R. M.; Pantano, C. G. *J. Appl. Phys*. **1990**, *68*, 4225.
(27) McDonald, R. S. *J. Am. Chem. Soc*. **1958**, *62*, 1168.
(28) Zecchina, S.; Bordiga, S.; Spoto, G.; Marchese, L.; Petrini, G.; Leofanti, G.; Padovan, M. *J. Phys. Chem*. **1992**, *96*, 4991.
(29) Morrow, B. A.; McFarlan, A. J. *Langmuir* **1991**, *7*, 1695.
(30) Fidalgo, A.; Nunes, T. G.; Ilharco, L. M. *J. Sol−Gel Sci. Technol*. **2000**, *19*, 403.
(31) Fidalgo, A.; Ilharco, L. M. *J. Non-Cryst. Solids* **2001**, *283*, 144.
(32) Van Beck, J. J.; Seykens, D.; Jansen, J. B. H.; Schuiling, R. D. *J. Non-Cryst. Solids* **1991**, *134*, 14.
(33) Yang, P.; Zhao, D.; Margolese, D. I.; Chmelka, B. F.; Stucky, G. D. *Chem. Mater*. **1999**, *11*, 2813.
(34) Christiansen, S. C.; Zhao, D.; Janicke, M. T.; Landry, C. C.; Stucky, G. D.; Chmelka, B. F. *J. Am. Chem. Soc*. **2001**, *123*, 4519.
(35) Sen, P. N.; Thorpe, M. F. *Phys. Rev. B* **1977**, *15*, 4030.
(36) Galeener, F. L. *Phys. Rev. B* **1979**, *19*, 4292.
(37) Almeida, R. M.; Vasconcelos, H. C. *SPIE* **1994**, *2288*, 678.
(38) Berreman, D. W. *Phys. Rev*. **1963**, *130*, 2193.
(39) Primeau, N.; Vautey, C.; Langlet, M. *Thin Solid Films* **1997**, *310*, 47.
(40) Kirk, C. T. *Phys. Rev. B* **1988**, *38*, 1255.
(41) Galeener, F. L.; Lucovsky, G. *Phys. Rev. Lett*. **1976**, *37*, 1474.
(42) Lange, P. *J. Appl. Phys*. **1989**, *66*, 201.
(43) Lange, P.; Windrabcke, W. *Thin Solid Films* **1989**, *174*, 159.
(44) Lange, P.; Schnakenberg, U.; Ullerich, S.; Schliwinski, H. J. *J. Appl. Phys*. **1990**, *68*, 3532.
(45) Perez-Robles, J. F.; Garcia-Cerda, L. A.; Espinoza-Beltran, F. J.; Yanez-Limon, M.; Gonzalez-Hernandez, J.; Vorobiev, Y. V.; Parga-Torres, J. R.; Ruiz, F.; Mendez-Nonell, J. *Phys. Status Solidi* **1999**, *172*, 49.
(46) Berquier, J. M.; Teyssedre, L.; Jacquiod, C. *J. Sol−Gel Sci. Technol*. **1998**, *13*, 739.
(47) Berquier, J. M.; Nael, P.; Jupille, J.; Jacquiod, C. *J. Sol−Gel Sci. Technol*. **2000**, *19*, 2000.
(48) Keene, M. T. J.; Gougeon, R. D. M.; Denoyel, R.; Harris, R. K.; Rouquerol, J.; Llwellyn, P. L. *J. Mater. Chem*. **1999**, *9*, 2843.